Hindawi Publishing Corporation
Journal of Nanomaterials
Volume 2009, Article ID 429867, 8 pages
doi:10.1155/2009/429867

Research Article

Electrical Transport Properties of $Ni_{95}Ti_5$ Catalyzed Multi wall Carbon Nanotubes Film

Zishan Husain Khan,[1,2] Numan Salah,[1] and Sami Habib[1]

[1] *Center of Nanotechnology, King Abdul Aziz University, P.O. Box 80216, Jeddah 21589, Saudi Arabia*
[2] *Department of Applied Sciences & Humanities, Faculty of Engineering &Technology, Jamia Millia Islamia (Central University), New Delhi, India*

Correspondence should be addressed to Zishan Husain Khan, zishan_hk@yahoo.co.in

Received 22 July 2008; Revised 22 October 2008; Accepted 4 March 2009

Recommended by Jun Li

Carbon nanotubes (CNTs) can be understood as one or more graphite sheets rolled up into a seamless cylinder. CNTs have gained much attention and scientific interest due to their unique properties and potential applications since their discovery in 1991. In the present work, we have deposited Ni95Ti5 film using thermal deposition method. Finally, the $Ni_{95}Ti_5$ catalyzed multi wall carbon nanotubes (MWNTs) are grown on silicon substrate using low pressure chemical vapor deposition (LPCVD) method and the electrical transport properties of this MWNTs film are studied over a temperature range (284–4K) to explain the conduction mechanism. We have suggested two types of conduction mechanism for the entire temperature range. For the temperature region (284–220K), the conduction is due to thermally activated process, whereas the conduction takes place via variable range hopping (VRH) for the temperature range of (220–4K). The VRH mechanism changes from three dimensions to two dimensions as we move down to the temperature below 50K. Therefore, the data for the temperature region (220–50K) is plotted for three dimensional variable range hopping (3D VRH) model and the two dimensional variable range hopping (2D VRH) for lower temperature range of (50–4K). These VRH models give a good fit to the experimental data. Using these models, we have calculated various interesting electrical parameters such as activation energy, density of states, hopping distance and hopping energy.

1. Introduction

Carbon nanotubes (CNTs) can be understood as one or more graphite sheets rolled up into a seamless cylinder. CNTs have gained much attention and scientific interest due to their unique properties [1] and potential applications [2–6] since their discovery in 1991 [7]. In general, electrical properties of nanotubes depend on the structure and the chirality [8–10]. Depending on the arrangement of carbon atoms, CNTs can be either metallic or semiconducting [8–10]. For semiconducting CNTs, the band gap is normally inversely proportional to the diameter [8, 9]. Thus, structure control of the CNTs is important in controlling the electrical properties of the CNTs. Furthermore, CNTs are excellent electrical candidates for nanoscale devices [11–16]. Due to high conductivity and the high-current density, multiwall carbon nanotubes (MWNTs) in particular have been considered for the use in wiring leads in future large-scale integration (LSI) circuits [17]. For this novel electronic system, there are many interesting properties expected in future. Some of the devices such as nanoscale diodes [11, 12, 15], field-effect transistors [13], and single-electron transistors (SETs) [14] using CNTs have been already demonstrated and characterized. On the other hand, the electrical transport properties of CNTs, which are basic electrical properties of the nanotubes, are not fully understood, although many efforts have been made. The metallic resistivity in single-wall nanotube (SWNT) crystalline ropes is observed by Fisher et al. [18]. Several groups have reported variable range hopping (VRH) conduction in carbon nanotubes (CNTs) [19–21]. In their results, the reports vary on the dimensionality of the VRH, ranging from one to three dimensions. It has also been reported that the three dimensional variable range

hopping can be observed, and the effect of the Coulomb gap is negligible. Moreover, there is a report indicating that acid treatment of SWNTs in carbon soots can promote changes from two-to-three dimensional VRH mechanisms [22]. Therefore VRH is quite commonly observed in CNTs and it is one of the important phenomena to be studied in detail to understand basic structure of this complex system.

In the present work, we have deposited $Ni_{95}Ti_5$ film using thermal deposition method. Here we have chosen titanium (Ti) to make an alloy with nickel (Ni) because it reduces oxidation of Ni which might occur during the exposure of film in air. Ti capping [23], Ti interlayer [24] or Ti alloying [25] has been reported to successfully tackle the problem of residual interfacial oxide. Due to its high affinity towards oxygen, Ti was found to out segregate to the surface and form TiO_x layer on the surface of the sample. It appears that TiO_x layer acts as a diffusion barrier to prevent the Ni from oxidizing. Finally, the $Ni_{95}Ti_5$ catalyzed multi wall carbon nanotubes (MWNTs) are grown on silicon substrate using low pressure chemical vapour deposition (LPCVD) method, and the electrical transport properties of this MWNTs film are studied over a temperature range 284–4 K to explain the conduction mechanism. We have suggested two types of conduction mechanism for the entire temperature range. For the temperature region 284–220 K, the conduction is due to thermally activated process, whereas the conduction takes place via variable range hopping (VRH) for the temperature range of 220–4 K. The VRH mechanism changes from three dimensions to two dimensions as we move down to the temperature below 50 K. Therefore, the data for the temperature region 220–50 K is plotted for three dimensional variable range hopping (3D VRH) model and the two dimensional variable range hopping (2D VRH) for lower temperature range of 50–4 K. These VRH models give a good fit to the experimental data. Using these models, we have calculated various interesting electrical parameters such as activation energy, density of states, hopping distance, and hopping energy.

2. Experimental

Low pressure chemical vapour deposition (LPCVD) method is used to fabricate CNTs on a nanocrystalline film of $Ni_{95}Ti_5$. These CNTs are produced by the catalytic deposition of C_2H_2 at 800°C, at a chamber pressure of 10 Torr. The growth time is kept fixed at 15 minutes. The gas mixtures of N_2 : C_2H_2 : H_2 with flow rates 300 : 50 : 50 sccm, respectively, are passed through the mass flow controllers (MFC's). The catalyst film of $Ni_{95}Ti_5$ is deposited on a silicon substrate using thermal vapour deposition method under an ambient argon pressure of 5 Torr. The morphology and microstructure of these CNTs are studied using Field Emission Scanning Electron Microscope (FESEM, JOEL 6500) and High Resolution Transmission Electron Microscope (HRTEM, JEOL- 264 JEM 3011) operated at 300 kV. The diameter and wall structure of these CNTs are studied using HRTEM. An Energy dispersive X-ray spectrometer (EDX) is used to verify presence of nickel (Ni) and titanium (Ti) on the nanocrystalline $Ni_{95}Ti_5$ catalyst film. We have employed a Raman Spectrophotometer (Bruker, RFS 100/s with Nd : YAG laser with an excitation wavelength of 1064 nm) to verify the structure of as-grown MWNTs. The electrical properties of these as-grown MWNTs are measured using standard four probe method over a temperature range of 284–4 K. For four probe methods, we have used platinum wires as probes. These wires are pasted with the help of silver paste on the as grown MWNTs film, and the distance between each contact is kept at 4 mm. A specially designed sample holder is used for these measurements. A standard lock-in technique is used to measure the temperature dependence of resistance over a temperature range of 284–4 K.

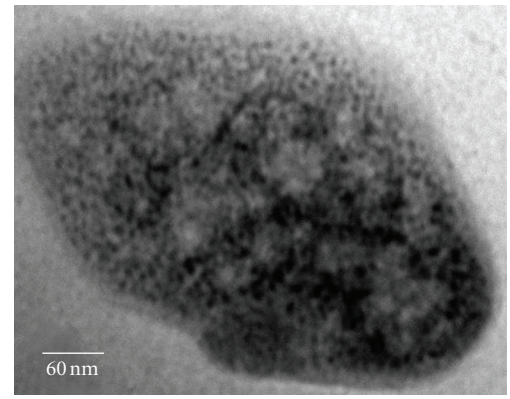

Figure 1: TEM image of nanocrystalline $Ni_{95}Ti_5$ catalyst.

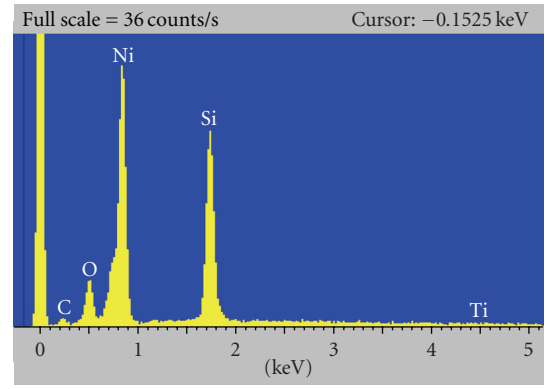

Figure 2: EDX spectra showing the presence of Ni and Ti.

3. Results and Discussion

Figure 1 represents the TEM image of the catalyst nanocrystalline film of the $Ni_{95}Ti_5$ deposited on silicon substrate. The size of these $Ni_{95}Ti_5$ nanoparticles varies from 5 to 10 nm. The composition of the $Ni_{95}Ti_5$ catalyst film is also analyzed using an energy dispersive X-ray spectroscopy (EDX). The EDX spectrum presented in Figure 2 suggests that the $Ni_{95}Ti_5$ film contains both Ni and Ti. To study the general morphology of carbon nanotubes (CNTs), we have

employed FESEM. Figures 3 and 4 show the FESEM images of CNTs grown on $Ni_{95}Ti_5$ catalyst film at low and high magnifications, respectively. The diameter of these nanotubes varies from 20 to 70 nm and, length of these CNTs is of the order of several hundred nanometers. The microstructure of these as grown CNTs is studied using transmission electron microscopy (TEM) and high-resolution transmission electron microscopy (HRTEM), respectively. Figure 5 shows the TEM image of these as grown CNTs. It is clear that these nanotubes are multi-walled and contains a lot of impurities/disorders. Figure 6 represents the HRTEM image of $Ni_{95}Ti_5$ catalyzed MWNT. The diameter of the center hollow portion of the MWNT is about 6 nm with the wall thickness of about 30 nm. These MWNTs do not possess a coaxial cylindrical structure but are made up of imperfect and broken graphite walls (shown in inset of Figure 6). The structure of the MWNT is not well graphitized, but it seems to be defective/disordered structure, which is also verified with the Raman spectrum of these MWNTs.

Raman spectrum is helpful in providing deep insight in the physical properties as well as the quality of material. This process does not only yield information not only about the vibrational properties but it is also deeply influenced by the electronic states of the system. In carbon nanotubes, Raman Spectroscopy is commonly used to verify the graphitic structure. Raman spectra of MWNTs grown on nanocrystalline $Ni_{95}Ti_5$ film are shown in Figure 7. In the present work, we have used a Raman Spectrophotometer (Bruker, RFS 100/s), using Nd:YAG laser with an excitation wavelength of 1064 nm. The spectra (Figure 7) clearly show weak peak at 1580 cm^{-1} (G-band), indicating the formation of less-graphitized MWNTs. The D mode (the disorder band), located between 1330–1360 cm^{-1}, is generally observed in CVD grown MWNTs. The intense peak observed at 1340 cm^{-1} (D-band) suggests that the amorphous carbonaceous particles adhered to MWNTs walls and defective pentagon and heptagon structures exist in the less-graphitized walls. Further, the ratio of the intensity of D band (I_D) and that of G-band (I_G) is good indicators of the quality of bulk sample. Normally the ratio I_D/I_G is quite high for a disordered system. In the present sample of MWNTs, G-band is at 1591 nm, and D-band is at 1340 nm and the ratio I_D/I_G is quite high ($\sim$ 1.12) which shows that these MWNTs contain a lot of defects.

Various models have been tried to explain nonlinear behaviour of resistance with temperature in carbon nanotubes. The responsible mechanisms for the decrease in conductance at lower temperatures in MWNTs containing a lot of impurities or disorder include thermally activated transport, variable range hopping, and weak localization [22, 26, 27]. In the present work, we have studied the temperature dependence of resistance of $Ni_{95}Ti_5$ catalyzed MWNTs over the temperature range of 284–4 K (Figure 8). It is observed that the entire data for the temperature region 284–4 K can also be fitted well with the help of the thermally activated and variable range hopping models. Here, we have explained the temperature dependence of conductivity using thermally activated process for the temperature region 284–220 K and variable range hopping for the temperature range 220–4 K.

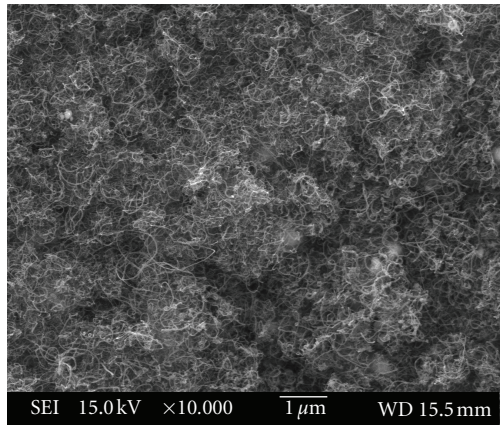

Figure 3: FESEM image of as-grown $Ni_{95}Ti_5$ catalyzed CNTs at low magnification (10 K).

Mott [28] has proposed the concept of variable range hopping (VRH) of localized electrons between the different sites for disordered systems. In this conduction process, electron hops between localized states with energy as low as possible. These states are kept far from each other involving certain distance, which is called hopping distance. This hopping distance increases with the decreasing temperature, which gives rise to the origin of 'variable range hopping (VRH)'. Therefore, the dependence of temperature on the electrical conductivity in the VRH regime is expressed as $\sigma(T) = \sigma_0 \exp[-(T_0/T)]^d$, where σ is the electrical conductivity, T is the temperature, σ_0 and T_0 are the constants, and d = 1/3, 1/4 for noninteracting two-dimensional (2D) and three-dimensional (3D) systems, respectively.

Figure 9 shows the plot of lnσ vs 1000/T for the temperature range of 284–220 K. It is observed that the plot of lnσ Vs 1000/T is straight line, which indicates that the conduction in this system is through thermally activated process. The conductivity can therefore be expressed by the usual relation:

$$\sigma = \sigma_0 \cdot \exp\left(-\frac{\Delta E}{k_B T}\right), \tag{1}$$

where ΔE is the activation energy and k_B is Boltzman constant. The value of ΔE calculated using slope of Figure 9 comes out to be 0.1491 eV. On the basis of calculated value of ΔE, we may suggest that conduction takes place in localized states for the temperature range 284–220 K in the present sample of $Ni_{95}Ti_5$ catalyzed MWNTs.

The experimental data based on the resistance-temperature measurements have been fitted for three- as well as two-dimensional variable range hopping (VRH) for the temperature region 220–4 K. It is found that the experimental data follows Mott's 3D VRH up to 50 K. Below 50 K, it follows 2D VRH model, that is, a crossover of conduction mechanism from the exp $[-(T_0/T)]^{1/4}$ law in the temperature range 220–50 K to exp$[-(T_m/T)]^{1/3}$ in the low temperature range 50–4 K is observed for the present sample of $Ni_{95}Ti_5$ catalyzed MWNTs. This behaviour is

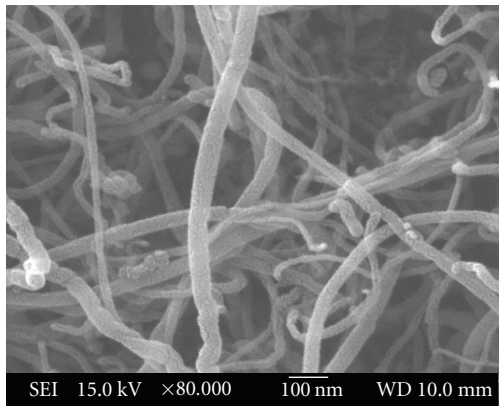

Figure 4: FESEM image of as grown $Ni_{95}Ti_5$ catalyzed CNTs at high magnification (80 K).

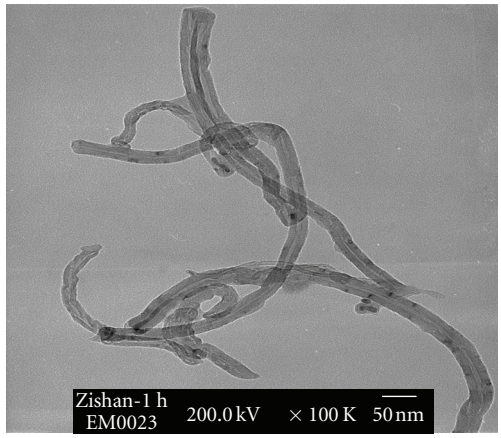

Figure 5: TEM image of as-grown $Ni_{95}Ti_5$ catalyzed MWNTs.

attributed to temperature-induced transition from three-dimension (3D) to two-dimension (2D) VRH. Moreover, it can also be explained on the basis of phonon energy available for the transport of the carriers, which will be reduced at lower temperatures for the transport of carriers for 2D VRH as compared to 3D VRH. The experimental data is divided into two different temperature ranges, that is, (220–50 K) for 3D VRH model and (50–4 K) for 2D VRH model.

Initially, we have replotted the experimental data for the temperature range 220–50 K as $\ln\sigma\sqrt{T}$ Vs $T^{-1/4}$ for 3D variable range hopping, which is presented in Figure 10. From this plot, it is clear that the conductivity increases slowly with increasing temperature over the temperature range 220–50 K, which suggests that the conduction is due to variable range hopping. This 3D VRH is characterized by the Mott [28–32] expression of the form

$$\sigma = \sigma_0 \cdot \exp\left[-\left(\frac{T_0}{T}\right)\right]^{1/4}, \tag{2}$$

where

$$T_o^{1/4} = \frac{\lambda\alpha^3}{kN(E_F)}. \tag{3}$$

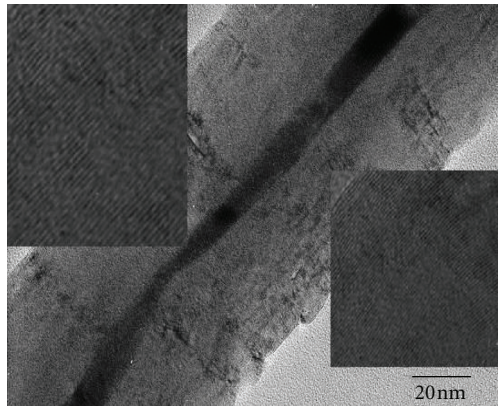

Figure 6: HRTEM image of as-grown $Ni_{95}Ti_5$ catalyzed MWNT (inset images showing broken graphite walls).

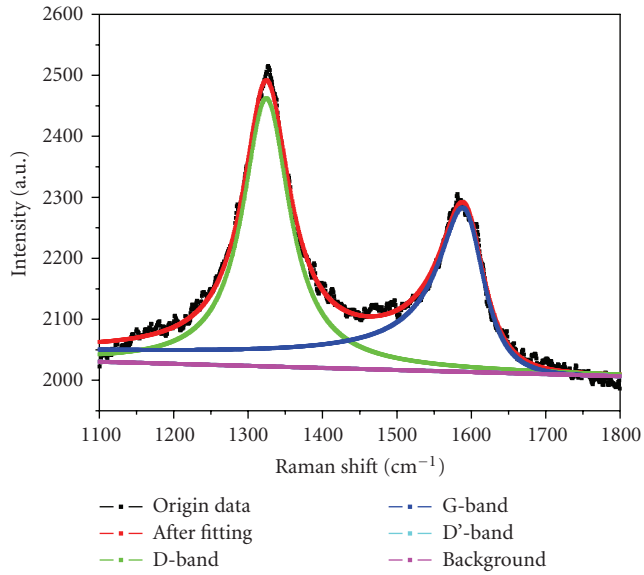

Figure 7: Raman spectra of as-grown $Ni_{95}Ti_5$ catalyzed CNTs.

$N(E_F)$ represents the density of localized states at E_F, λ is a dimensionless constant (about 18), α^{-1} is the spatial extension of the wave function $\exp(-\alpha R)$ associated with the localized states, T_0 represents the degree of disorder, and k is the Boltzmann constant. The value of σ_o as obtained by various workers is given by

$$\sigma_o = 3e^2\gamma\left(\frac{N(E_F)}{8\pi\alpha kT}\right)^{1/2}. \tag{4}$$

where e is the electron charge and γ is the Debye frequency (about 10^{13} Hz).

Simultaneous solution of (2) and (3) yields

$$\alpha = 22.52 \cdot \sigma \cdot T_o^{1/2}\text{cm}^{-1}. \tag{5}$$

$$N(E_F) = 2.12 \times 10^9\sigma_o^3 \cdot T_o^{1/2}\text{cm}^{-3}\text{eV}^{-1}. \tag{6}$$

The hopping distance [28–32] is given by

$$R = \left(\frac{9}{8\pi\alpha kTN(E_F)}\right)^{1/4}. \quad (7)$$

Hopping energy is also given by [28–32]

$$W = \left(\frac{3}{4\pi R^3 N(E_F)}\right). \quad (8)$$

On the basis of fitting with Mott's three dimensional variable hopping model, we have calculated various parameters, such as density of states ($N(E_F)$), degree of disorder (T_o), hopping distance (R), and hopping energy (W) with the help of equations (2–8). These parameters are called Mott's parameters. For variable range hopping, the value of W should be of the order of few k_BT, and αR should be greater than unity, or of the order of unity, as suggested by Mott. The values of these Mott's parameters are shown in Table 1. It is evident from this table that the calculated values of W and αR are of the order of the few k_BT and unity respectively, which shows close agreement with Mott's variable range hopping [28–32]. It is also found that the hopping distance increases with the decrease in temperature, while the hopping energy decreases with the decrease in temperature. The density of states near the Fermi level extracted from VRH parameters is estimated to be 1.67×10^{26} eV^{-1} cm^{-3}. Several workers have reported the bulk density of states, a typical value of amorphous carbon films $\approx$ 10^{18} eV^{-1} cm^3 [33–35]. For one-layer carbon nanotube films, the density of states at Fermi level was estimated to be $\approx$ 10^{21} eV cm^{-3} [36]. Recently Aggarwal et al. [37] reported the density of states as high as 10^{24} eV^{-1} cm^{-3} for Fe-Pd catalyzed MWNTs film. Here, we have reported the electrical transport properties of MWNTs film which is a bulk sample containing thousands of nanotubes. In the present system, the value of $N(E_F)$ is a little higher than that of the reported values on MWNTs film. Here, the disorderedness does not only come from amorphous carbon, but also from the defective structure of MWNTs, which results in high value of density of defect states. Therefore, not only is the amorphous carbon deposited on the sample during growth process, but also the highly disorder structure of MWNTs is responsible for high value of density of states. The presence of more amorphous carbon on the sample is confirmed by Raman spectroscopy, whereas, the defective structure of these as grown MWNTs is verified by HRTEM image. The degree of disorder (T_o) is estimated to be 0.6512×10^4 K. Various workers have reported the value of $T_o \approx 10^4$ K for plasma-polymerized C_{60} thin films [38] and, on the basis of the value of T_o, they concluded that their system is disordered. In our case, the value of T_o is of the same order as that of the reported by these workers, which suggests that the present sample of $Ni_{95}Ti_5$ catalyzed MWNTs contains lots of disorderedness. This is also verified by HRTEM image and Raman spectra of MWNTs.

At very low temperatures, the conductivity is further suppressed and increases very slowly with the increasing temperature for the lower temperature region of 50–4 K. We have fitted our experimental data well with Mott's 2D variable range hopping for the lower temperature. On the

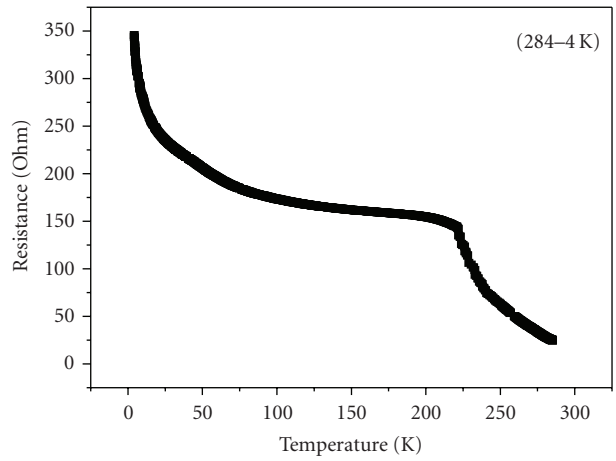

Figure 8: Resistance vs Temperature plot for as grown $Ni_{95}Ti_5$ catalyzed CNTs (284–4 K).

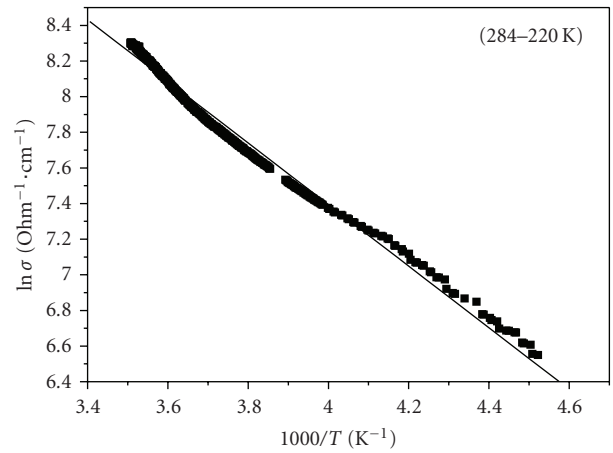

Figure 9: lnσ vs 1000/T for as grown $Ni_{95}Ti_5$catalyzed MWNTs (284–220 K).

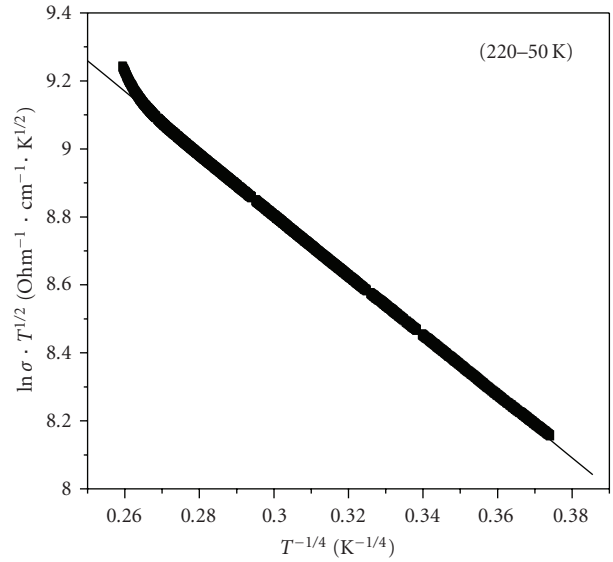

Figure 10: ln $(\sigma\sqrt{T})$ vs $T^{-1/4}$ plot for as grown $Ni_{95}Ti_5$ catalyzed MWNTs (220–50 K).

Table 1: The Mott parameters for temperature range 220–50 K.

T(K)	$N(E_F)$ ($eV^{-1}cm^{-3}$)	T_o (K)	α (cm^{-1})	R (cm)	W (meV)	αR
220	1.67×10^{26}	0.6512×10^4	1.803×10^8	5.004×10^{-9}	11.42	0.902
180	1.67×10^{26}	0.6512×10^4	1.803×10^8	5.262×10^{-9}	9.82	0.949
140	1.67×10^{26}	0.6512×10^4	1.803×10^8	5.603×10^{-9}	8.13	1.0103
100	1.67×10^{26}	0.6512×10^4	1.803×10^8	6.095×10^{-9}	6.32	1.099
50	1.67×10^{26}	0.6512×10^4	1.803×10^8	7.248×10^{-9}	3.76	1.307

basis of this fitting, it is suggested that conduction is due to 2D variable range hopping in localized states near the Fermi level. Therefore, the experimental data have been re-plotted as lnσ versus $T^{-1/3}$ for 2D VRH.

Figure 11 represents the plot of ln σ versus $T^{-1/3}$ in the temperature range (50–4 K). It shows that all the data points almost form a straight line, indicating that conductivity (σ) obeys the following equation:

$$\sigma = \sigma_0 \cdot \exp\left[-\left(\frac{T_m}{T}\right)\right]^{1/3} \tag{9}$$

The linear behaviour of lnσ vs. $T^{-1/3}$ plot suggests that the conduction is due to Mott's two-dimensional (2D) noninteracting variable range hopping, which is consistent with the disordered structure of the present sample of $Ni_{95}Ti_5$ catalyzed MWNTs. HRTEM image shown in Figure 6 also suggests that the carbon nanotubes do not possess a long-range order, but it contains imperfect graphite layers of varying sizes. This is further verified by Raman spectra of as grown MWNTs (Figure 7). A Raman spectrum shows an intense D-band peak, indicating that the sample contains lots of impurities and defects. Gao et al [39] also reported the similar observations for multi-walled carbon nanotubes. Therefore it is suggested that the transport along a continuous single shell or set of shells as in the case of MWNTs is impossible and only the disordered structure of MWNT plays important role. Therefore, it may be suggested that the disorder localizes the electronic wave function, thus giving rise to variable range hopping.

In two-dimensional variable range hopping regime, the characteristic temperature (T_m) is related to the density of states at the Fermi level $N(E_F)$ and the localization length ξ as [40]

$$T_m = \frac{13.8}{k_B N(E_F)\xi^2}. \tag{10}$$

And the temperature dependence of optimum hopping distance is given by

$$R(T) = \frac{1}{3}\xi\left(\frac{T_m}{T}\right)^{1/3}. \tag{11}$$

The localization length and the optimum hopping distance for these disordered MWNTs have been estimated using relations (9)-(10). We have used the value of $N(E_F)$ estimated using 3D VRH as suggested by earlier workers [41] to calculate the localization length and hopping distance. The localization length is calculated to be 0.334×10^{-9} cm using the value of T_m and the density of states $N(E_F)_{3D}$. This gives an optimum hopping distance of 0.043×10^{-9} cm and 0.098×10^{-9} cm at 50 and 4 K, respectively.

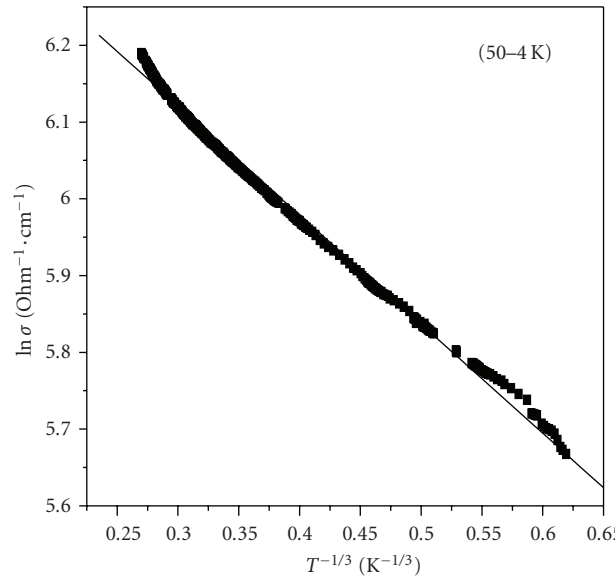

Figure 11: lnσ vs $T^{-1/3}$ plot for as grown $Ni_{95}Ti_5$ catalyzed MWNTs. (50–4 K).

4. Conclusion

From the above results and discussion, it is concluded that the conduction mechanism in the present sample of $Ni_{95}Ti_5$ catalyzed MWNTs is explained with the help of two models, that is, thermally activated process for the temperature range of 284–220 K and variable range hopping for the temperature range of 220–4 K. For thermally activated process, we have calculated the activation energy, which comes out to be 0.1491 eV. On the basis of calculated value of ΔE, we suggest that conduction takes place in localized states for the temperature range 284–220 K in the present sample of $Ni_{95}Ti_5$ catalyzed MWNTs. Variable range hopping is suggested to be responsible for the transport of charge carriers for the low temperature range of 220–4 K. This variable range hopping changes from 3D to 2D for the much lower temperature region 50–4 K. Using 3D VRH model, the calculated values of Mott's parameters for the present sample of $Ni_{95}Ti_5$ catalyzed MWNTs are encouraging and also satisfy the condition of Mott's variable range hopping (W of the order few k_BT and αR should be of the order of/greater than

unity). For these MWNTs, the hopping distance has also been calculated using 2D Mott's VRH model. The value of hopping distance varies from 0.043×10^{-9} cm to 0.098×10^{-9} cm as the temperature decreases from 50 to 4 K. This hopping behavior is consistent with the highly disordered structure of MWNTs studied here. These MWNTs do not possess a coaxial cylindrical structure, but are made up of imperfect and broken graphite cylinders of varying sizes. Hence transport along a single continuous shell or set of shells as in the case of well-graphitized MWNT is impossible. Therefore, conduction will take place only along the surface of these MWNTs.

References

[1] M. S. Dresselhaus, "Down the straight and narrow," *Nature*, vol. 358, no. 6383, pp. 195–196, 1992.

[2] C. N. R. Rao, B. C. Satishkumar, A. Govindaraj, and M. Nath, "Nanotubes," *ChemPhysChem*, vol. 2, no. 2, pp. 78–105, 2001.

[3] B. C. Satishkumar, A. Govindaraj, and C. N. R. Rao, "Bundles of aligned carbon nanotubes obtained by the pyrolysis of ferrocene-hydrocarbon mixtures: role of the metal nanoparticles produced in situ," *Chemical Physics Letters*, vol. 307, no. 3-4, pp. 158–162, 1999.

[4] W. A. de Heer, A. Châtelain, and D. Ugarte, "A carbon nanotube field-emission electron source," *Science*, vol. 270, no. 5239, pp. 1179–1180, 1995.

[5] D. S. Bethune, C. H. Kiang, M. S. de Vries, et al., "Cobalt-catalysed growth of carbon nanotubes with single-atomic-layer walls," *Nature*, vol. 363, no. 6430, pp. 605–607, 1993.

[6] A. C. Dillon, K. M. Jones, T. A. Bekkedahl, C. H. Kiang, D. S. Bethune, and M. J. Heben, "Storage of hydrogen in single-walled carbon nanotubes," *Nature*, vol. 386, no. 6623, pp. 377–379, 1997.

[7] S. Iijima, "Helical microtubules of graphitic carbon," *Nature*, vol. 354, no. 6348, pp. 56–58, 1991.

[8] R. Saito, G. Dresselhaus, and M. S. Dresselhaus, *Physical Properties of Carbon Nanotubes*, chapters 3-4, Imperial College Press, London, UK, 1998.

[9] M. S. Dresselhaus, G. Dresselhaus, and P. C. Eklund, *Science of Fullerenes and Carbon Nanotubes*, chapter 19, Academic Press, San Diego, Calif, USA, 1996.

[10] R. Saito, M. Fujita, G. Dresselhaus, and M. S. Dresselhaus, "Electronic structure of chiral graphene tubules," *Applied Physics Letters*, vol. 60, no. 18, pp. 2204–2206, 1992.

[11] Z. Yao, H. W. Ch. Postma, L. Balents, and C. Dekker, "Carbon nanotube intramolecular junctions," *Nature*, vol. 402, no. 6759, pp. 273–276, 1999.

[12] L. Chico, V. H. Crespi, L. X. Benedict, S. G. Louie, and M. L. Cohen, "Pure carbon nanoscale devices: nanotube heterojunctions," *Physical Review Letters*, vol. 76, no. 6, pp. 971–974, 1996.

[13] S. J. Tans, A. R. M. Verschueren, and C. Dekker, "Room-temperature transistor based on a single carbon nanotube," *Nature*, vol. 393, no. 6680, pp. 49–52, 1998.

[14] M. Bockrath, D. H. Cobden, P. L. McEuen, et al., "Single-electron transport in ropes of carbon nanotubes," *Science*, vol. 275, no. 5308, pp. 1922–1925, 1997.

[15] T. W. Ebbesen, H. J. Lezec, H. Hiura, J. W. Bennett, H. F. Ghaemi, and T. Thio, "Electrical conductivity of individual carbon nanotubes," *Nature*, vol. 382, no. 6586, pp. 54–56, 1996.

[16] C. Dekker, "Carbon nanotubes as molecular quantum wires," *Physics Today*, vol. 52, no. 5, pp. 22–28, 1999.

[17] N. Aoki, J. Takayama, M. Kida, et al., "Bonding process for nanoscale wiring using carbon nanotube by STM tip," *Japanese Journal of Applied Physics*, vol. 42, no. 4B, pp. 2419–2421, 2003.

[18] J. E. Fischer, H. Dai, A. Thess, et al., "Metallic resistivity in crystalline ropes of single-wall carbon nanotubes," *Physical Review B*, vol. 55, no. 8, pp. R4921–R4924, 1997.

[19] Y. Yosida and I. Oguro, "Variable range hopping conduction in bulk samples composed of single-walled carbon nanotubes," *Journal of Applied Physics*, vol. 86, no. 2, pp. 999–1003, 1999.

[20] Z. K. Tang, H. D. Sun, and J. Wang, "Electrical transport properties of mono-dispersed single-wall carbon nanotubes formed in channels of zeolite crystal," *Physica B*, vol. 279, no. 1–3, pp. 200–203, 2000.

[21] S. Bandow, S. Numao, and S. Iijima, "Variable-range hopping conduction in the assembly of boron-doped multiwalled carbon nanotubes," *Journal of Physical Chemistry C*, vol. 111, no. 32, pp. 11763–11766, 2007.

[22] B. Liu, T. Wågberg, E. Olsson, et al., "Synthesis and characterization of single-walled nanotubes produced with Ce/Ni as catalysts," *Chemical Physics Letters*, vol. 320, no. 3-4, pp. 365–372, 2000.

[23] W. L. Tan, K. L. Pey, S. Y. M. Chooi, J. H. Ye, and T. Osipowicz, "Effect of a titanium cap in reducing interfacial oxides in the formation of nickel silicide," *Journal of Applied Physics*, vol. 91, no. 5, pp. 2901–2909, 2002.

[24] W. L. Tan, K. L. Pey, S. Y. M. Chooi, and J. H. Ye, "A comparative study of nickel silicide formation using a titanium cap layer and a titanium interlayer," in *Proceedings of the Materials Research Society Symposium*, vol. 670, pp. K661–K666, San Francisco, Calif, USA, April 2001.

[25] R. T. P. Lee, D. Z. Chi, M. Y. Lai, N. L. Yakovlev, and S. J. Chua, "Effects of Ti incorporation in Ni on silicidation reaction and structural/electrical properties of NiSi," *Journal of the Electrochemical Society*, vol. 151, no. 9, pp. G642–G647, 2004.

[26] W. Y. Jang, N. N. Kulkarni, C. K. Shih, and Z. Yao, "Electrical characterization of individual carbon nanotubes grown in nanoporous anodic alumina templates," *Applied Physics Letters*, vol. 84, no. 7, pp. 1177–1179, 2004.

[27] J. Kong, C. Zhou, A. Morpurgo, et al., "Synthesis, integration, and electrical properties of individual single-walled carbon nanotubes," *Applied Physics A*, vol. 69, no. 3, pp. 305–308, 1999.

[28] N. F. Mott and E. A. Davis, *Electronic Processes in Non-Crystalline Materials*, Clarendon Press, Oxford, UK, 1970.

[29] N. F. Mott, "Conduction in non-crystalline systems IV. Anderson localization in a disordered lattice," *Philosophical Magazine*, vol. 22, no. 175, pp. 7–29, 1970.

[30] E. A. Davis and N. F. Mott, "Conduction in non-crystalline systems V. Conductivity, optical absorption and photoconductivity in amorphous semiconductors," *Philosophical Magazine*, vol. 22, no. 179, pp. 903–922, 1970.

[31] N. F. Mott, E. A. Davis, and R. A. Street, "States in the gap and recombination in amorphous semiconductors," *Philosophical Magazine*, vol. 32, no. 5, pp. 961–996, 1975.

[32] N. F. Mott, "Conduction in non-crystalline materials III. Localized states in a pseudogap and near extremities of conduction and valence bands," *Philosophical Magazine*, vol. 19, no. 160, pp. 835–852, 1969.

[33] J. J. Hauser, "Electrical, structural and optical properties of amorphous carbon," *Journal of Non-Crystalline Solids*, vol. 23, no. 1, pp. 21–41, 1977.

[34] Th. Frauenheim, U. Stephan, K. Bewilogua, F. Jungnickel, P. Blaudeck, and E. Fromm, "Electrical transport and electronic properties of a amorphous carbon thin films," *Thin Solid Films*, vol. 182, no. 1-2, pp. 63–78, 1989.

[35] C. Godet, "Hopping model for charge transport in amorphous carbon," *Philosophical Magazine B*, vol. 81, no. 2, pp. 205–222, 2001.

[36] V. I. Tsebro, O. E. Omel'yanovskii, E. F. Kukovitskii, N. A. Sainov, N. A. Kiselev, and D. N. Zakharov, "Temperature dependence of electric resistance and magnetoresistance of pressed nanocomposites of multilayer nanotubes with the structure of nested cones," *Journal of Experimental and Theoretical Physics*, vol. 86, no. 6, pp. 1216–1219, 1998.

[37] M. Aggarwal, M. Husain, S. Khan, and Z. H. Khan, "Electrical conduction mechanism in $Fe_{70}Pd_{30}$ catalyzed multi-walled carbon nanotubes," *Journal of Nanoparticle Research*, vol. 9, no. 6, pp. 1047–1055, 2007.

[38] M. Shiraishi, M. Ramm, and M. Ata, "The characterization of plasma-polymerized C_{60} thin films," *Applied Physics A*, vol. 74, no. 5, pp. 613–616, 2002.

[39] H. Gao, C. Mu, F. Wang, et al., "Field emission of large-area and graphitized carbon nanotube array on anodic aluminum oxide template," *Journal of Applied Physics*, vol. 93, no. 9, pp. 5602–5605, 2003.

[40] B. I. Shklovskii and A. L. Efros, *Electronic Properties of Doped Semiconductors*, Springer, Berlin, Germany, 1984.

[41] W. Y. Jang, N. N. Kulkarni, C. K. Shih, and Z. Yao, "Electrical characterization of individual carbon nanotubes grown in nanoporous anodic alumina templates," *Applied Physics Letters*, vol. 84, no. 7, pp. 1177–1179, 2004.